

## Differential Rotational Soft X-Ray Tomography of Coupled MHD Modes

M. Sokoll, M. Bessenrodt-Weberpals and the ASDEX Upgrade Team  
Max-Planck-Institut für Plasmaphysik, EURATOM-Association,  
D-85748 Garching, Germany

### 1. Introduction

Soft X-rays (SXR) emitted from a fusion plasma can be used to diagnose and interpret magnetohydrodynamic (MHD) plasma activities and their structure. At the tokamak ASDEX Upgrade the soft X-radiation is measured by 5 pinhole cameras with a total of 124 detectors. The detected signals are integrals along lines-of-sight, which lie in one poloidal cross-section of the tokamak. Thus, a tomographic reconstruction is a very important tool for the interpretation of the data.

For investigation of complex mode structures (higher poloidal mode number, several modes) the spatial resolution is too poor due to the low number of detectors ( $\sim 10^2$ ), because of restricted space. On the other hand in the medical tomography some  $10^5$  chords are available [1].

To obtain sufficient spatial resolution tomography methods are adapted to the conditions in fusion plasmas. The method presented here is unique in its ability to reconstruct the soft X-ray emissivity of coupled MHD modes with high spatial resolution.

### 2. Differential Rotational Tomography

To improve the spatial resolution the well known method of rotational tomography can be used [2,3]. Here, time information is transformed into spatial information. Because of the toroidal and/or poloidal plasma rotation the mode rotates in the observation plane. Assuming a circular, rigid and concentric rotation of a stationary mode with constant angular velocity it is easy to correlate the data for one chord at different time points with the data for different chords at one time point.

To analyse noncircular and nonconcentric plasma shapes the rotational tomography was expanded by using an adaptive coordinate system  $(\rho, \varphi, \theta^*)$ .  $\rho$  is the radial poloidal flux coordinate. The toroidal coordinate  $\varphi$  is the Euclidean toroidal angle. The poloidal coordinate  $\theta^*$  is the straight field line angle, i. e., the magnetic field lines are straight in the plane  $(\varphi, \theta^*)$ . The definitions are as follows:

$$\rho = \sqrt{\frac{\psi - \psi_A}{\psi_S - \psi_A}}, \quad \theta^* \sim \int_0^\theta d\theta' \frac{1}{R} \frac{\partial(R, z)}{\partial(\psi, \theta')} \quad \text{for } \rho = \text{const.} \quad (1)$$

$\theta^*$  is normalized to  $2\pi$ .  $R$  and  $z$  are the Cartesian coordinates in the poloidal plane.  $\theta$  is the Euclidean poloidal angle.  $\psi$  is the poloidal flux obtained from equilibrium calculations. It takes the value  $\psi_S$  on the separatrix and  $\psi_A$  on the magnetic axis. All lines-of-sight lie in the plane  $(\rho, \theta^*)$  (or  $(R, z)$ ) at one toroidal location ( $\varphi=0$ ). The advantage of the coordinate system  $(\rho, \theta^*)$  is that the motion of one mode is represented as a rigid, uniform, circular and concentric rotation. This simple properties are offset by complex representation of the lines-of-sight in these coordinates, confer figure 1.

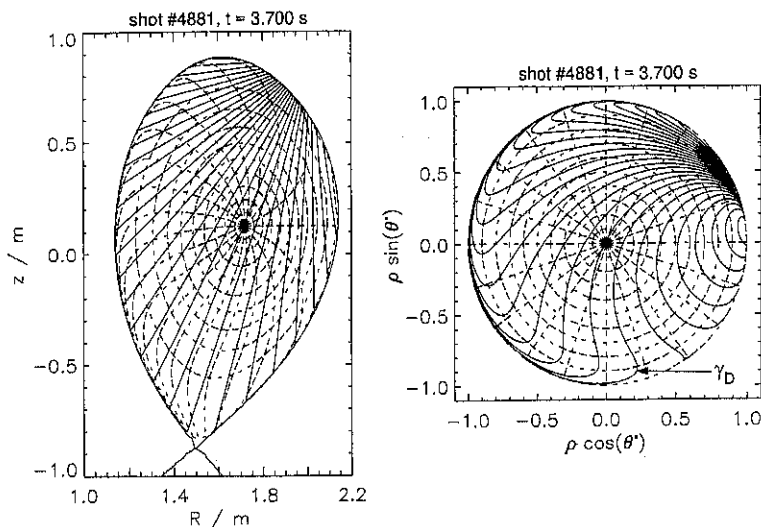


**Figure 1:** Lines of constant  $\rho$  and  $\theta^*$  (dashed), and lines-of-sight for camera D (solid), depicted in Euclidean (left) and adaptive (right) coordinates.

Conventional rotational tomography fails if more than one mode is present. To deal with this difficulty we developed two complementary strategies. First, if the modes are uncoupled, i. e. if they correspond to different frequencies in the measured signal, we separate them in the Fourier space using the fast Fourier transform (FFT). Second, if they are coupled, we apply an ansatz which takes into account the corresponding different rotational velocities in the observation plane ( $\rho, \theta^*$ ). This will be developed step by step in the following paragraphs.

First, look at the ansatz for the soft X-ray emissivity of a pure harmonic mode ( $m, n$ ):

$$g(\rho, \varphi, \theta^*) = A(\rho) e^{i(m\theta^* - n\varphi)} \quad (2)$$

Here,  $A(\rho)$  is the complex radial function of this mode. Its absolute part corresponds to the radial amplitude function. Next, assume a rigid plasma rotation with the frequency  $\omega$  and consider the time dependent ansatz at the toroidal location of the SXR diagnostic:

$$g(\rho, t, \theta^*) = A(\rho) e^{i(m\theta^* + n\omega t)} \quad (3)$$

The frequency  $\omega = \omega_{tor} - \frac{m}{n} \omega_{pol}$  is composed of the toroidal and poloidal plasma rotation. Now, expand this ansatz to different frequencies  $\omega_k$  and suppose for each of them a set of modes ( $m_{jk}, n_{jk}$ ):

$$g(\rho, t, \theta^*) = \sum_{jk} A_{jk}(\rho) e^{i(m_{jk}\theta^* + n_{jk}\omega_k t)} \quad (4)$$

For each mode there is one radial function  $A_{jk}(\rho)$ . It is defined as an arbitrary cubic spline with  $h$  internal knots. Thus, it can be represented as a linear combination of real and well defined cubic B-splines [4]:

$$A_{jk}(\rho) = \sum_{l=1}^{h+4} c_{jkl} N_{jkl}(\rho) \quad (5)$$

Equations 4 and 5 give the total ansatz

$$g(\rho, t, \theta^*) = \sum_{jkl} c_{jkl} N_{jkl}(\rho) e^{i(m_{jk}\theta^* + n_{jk}\omega_k t)} \quad (6)$$

The measured signal  $f_D(t)$  of a detector  $D$  is a line integral along a line-of-sight described by the curve  $\gamma_D$  (see figure 1):

$$f_D(t) = \sum_{jkl} c_{jkl} \left[ \int_{\gamma_D} ds N_{jkl}(\rho) e^{im_{jk}\theta^*} \right] e^{in_{jk}\omega_k t} =: \sum_{jkl} c_{jkl} I_{jklD} e^{in_{jk}\omega_k t} \quad (7)$$

This set of equations separates in the Fourier space with respect to  $\omega := n_{jk}\omega_k$ :

$$\hat{f}_D(\omega) = \sum_{jkl} c_{jkl} I_{jklD} \delta(n_{jk}\omega_k - \omega) \quad (8)$$

Thus, for each  $\omega$  we obtain one set of complex and linear equations.  $I_{jklD}$  depends only on the geometry of the diagnostic and on the coordinates  $\rho$  and  $\theta^*$ .  $c_{jkl}$  are unknown and  $\hat{f}_D(\omega)$  are values from the Fourier transform of the measured SXR data. Solving equations (8) for  $c_{jkl}$  and substituting it in equation (6) one obtain the unknown emissivity  $g$ .

Furthermore, we investigated errors and limits of our method. There are three main sources of errors: the measured line integrated intensities, the assumed geometry of the diagnostic and finally the magnetic equilibrium. The influence of these errors were investigated by tests, Monte Carlo simulations and calculations of error propagation. The approximate values of possible errors are listed in table 1, where the time variable emissivity  $\Delta g$  means the difference between the total emissivity  $g$  and the time independent emissivity, i. e. the (0,0) mode.

	$g$	$\Delta g$
measured intensity	1%	1%
geometry	0.5%	2%
equilibrium	2%	9%

**Table 1:** Approximate values of possible errors of the emissivity  $g$  and  $\Delta g$ .

For the splines we use mostly 11 knots ( $\rho=0.0, 0.1, 0.2, \dots, 1.0$ ). It corresponds to a radial resolution of about 5 cm ( $\Delta\rho=0.1$ ) for each mode. The poloidal resolution is limited by the number of harmonics, i. e. by the band width of the data acquisition system. This is large enough, so that the poloidal resolution is limited only by the spatial extension of the lines-of-sight, which corresponds to a resolution of about 4 cm.

### 3. Results

With this new high resolution method we investigated the internal kink, the evolution of the sawtooth crash, the growth of the tungsten snake and coupled modes. An example for the studies of coupled mode structures in ASDEX Upgrade high- $\beta$  discharges is shown in figure 2 [5]. Tomographic reconstructions of three phases of the discharge are depicted. In the first phase (left plots) the plasma does not reach the  $\beta$ -limit yet and a (1,1) mode is unstable. The radial mode amplitude and the contour plot of the time variable emissivity  $\Delta g$  can be seen. The next phase is at the beginning of the  $\beta$ -collapse. Here, we discovered a (4,3) mode with a toroidally coupled (3,3) mode. Finally, in the last phase during the  $\beta$ -collapse we reconstructed a (3,2) mode with a toroidally coupled (2,2) mode. The tomography procedure yields the  $m$  numbers while the  $n$  numbers are determined by the relations of the frequencies and by the Mirnov signals.

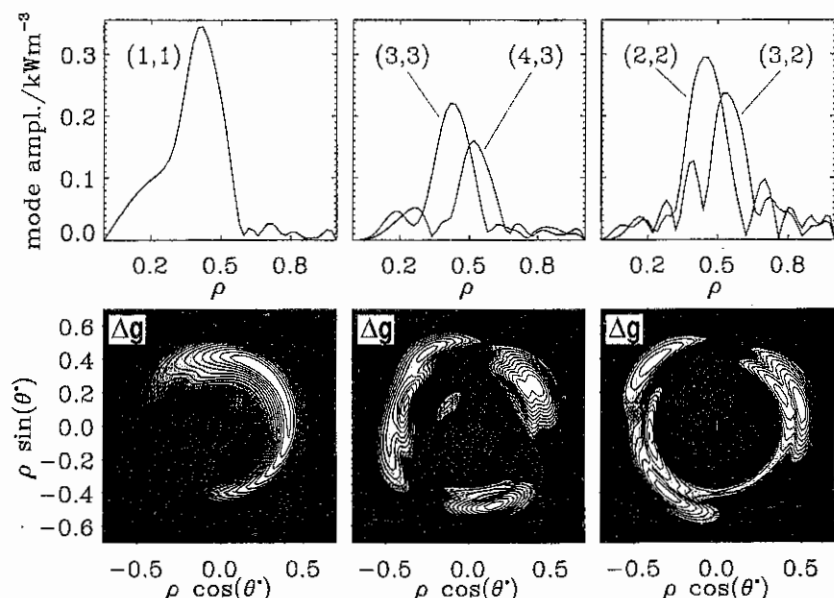


**Figure 2:** Tomographic reconstruction of an high- $\beta$  discharge in ASDEX Upgrade (shot #7694). Top: radial mode amplitudes. Bottom: contour plots of the time variable emissivity  $\Delta g$ . Left ( $t = 1.831$  s): (1,1) mode before the  $\beta$ -collapse. Middle ( $t = 1.844$  s): coupling of (4,3) and (3,3) modes at the beginning of the  $\beta$ -collapse. Right ( $t = 1.887$  s): coupling of (3,2) and (2,2) modes at the end of the  $\beta$ -collapse.

#### 4. Summary

An innovative tomography method was developed for interpretation of the soft X-ray data. It has high spatial resolution. For the first time, it is possible to reconstruct the soft X-ray emissivity of coupled MHD modes. The necessary assumption is a stationary mode structure on the time scale of one plasma rotation period (in ASDEX Upgrade:  $\sim 100 \mu\text{s}$ ). The main features are the use of rotational tomography in an adaptive coordinate system, an ansatz for coupled modes with the help of cubic splines and calculation in the Fourier space. Thereby the mode structures in high- $\beta$  discharges have been clarified in detail.

#### References

- [1] R. S. Granetz, P. Smeulders, *Nuclear Fusion* **28**, pp. 457, 1988
- [2] N. R. Sauthoff, S. von Goeler, *IEEE Transactions on Plasma Science* **PS-7**, pp. 141, 1979
- [3] Y. Nagayama, A. W. Edwards, *Review of Scientific Instruments* **63**, pp. 4757, 1992
- [4] H. B. Curry, I. J. Schoenberg, *Journal d'Analyse Mathématique* **17**, pp. 71, 1966
- [5] M. Sokoll *et al.*, to be published